IV. Conclusions

For the range of the angles of attack studied, the time-averaged mean distance to the onset of vortex breakdown on a pitching delta wing can be extended by nearly 100% with combined deflection of leading-edge flaps and transient trailing-edge blowing, which is invoked during only a fraction of the pitching cycle. Most effective is blowing during the upstroke portion of the cycle. With this approach, the effective momentum coefficient of the blowing is extremely small. Further optimization of controls will require detailed knowledge of the qualitative and quantitative character of the changes in the flow topology caused by the application of leading- and trailing-edge controls. This experiment is currently under way.

Acknowledgments

The authors are grateful to the U.S. Air Force Office of Scientific Research for support of this research under Grant F49620-95-1-0220 monitored by Len Sakell.

References

[1]Magness, C., Robinson, O., and Rockwell, D., "Control of Leading-Edge Vortices on a Delta Wing," AIAA Paper 89-0999, March 1989.

[2]Cipolla, K., and Rockwell, D., "Flow Structure on a Stalled Delta Wing Subjected to Small Amplitude Pitching Oscillations," *AIAA Journal*, Vol. 33, No. 7, 1995, pp. 1256–1262.

[3]Visbal, M. R., "Structure of Vortex Breakdown on a Pitching Delta Wing," AIAA Paper 93-0434, Jan. 1993.

[4]Rockwell, D., "Three-Dimensional Flow Structure on Delta Wings at High Angle-of-Attack: Experimental Concepts and Issues," AIAA Paper 93-0550, Jan. 1993.

[5]Gu, W., Robinson, O., and Rockwell, D., "Control of Vortices on a Delta Wing by Leading-Edge Injection," *AIAA Journal*, Vol. 31, No. 7, 1993, pp. 1177–1185.

[6]Helin, H. E., and Watry, C. W., "Effects of Trailing-Edge Jet Entrainment on Delta Wing Vortices," *AIAA Journal*, Vol. 32, No. 4, 1994, pp. 802–804.

Explicit Algebraic Stress Model of Turbulence with Anisotropic Dissipation

Xiang-Hua Xu* and Charles G. Speziale†
Boston University, Boston, Massachusetts 02215

I. Introduction

TURBULENT flows near solid boundaries—or at low turbulence Reynolds numbers—can exhibit significant anisotropies in the turbulent dissipation rate.[1] Nevertheless, Reynolds stress turbulence closures are routinely formulated that neglect such effects by invoking the Kolmogorov assumption of local isotropy.[2] Recently, however, attempts have been made to extend full Reynolds stress turbulence closures to incorporate the effects of anisotropic dissipation.[3–6] These more sophisticated Reynolds stress turbulence closures can involve the solution of up to 12 additional transport equations. As such, most of these models are not currently feasible for the solution of complex turbulent flows in an engineering setting.

During the past few years, explicit algebraic stress models have been developed that are formally consistent with full second-order closures in the limit of homogeneous turbulence in equilibrium.[7] These models allow for the solution of complex turbulent flows with a substantially reduced level of computation compared with full second-order closures, since they constitute two-equation models.[7,8] The purpose of the present Note is to show how the effects of anisotropic dissipation can be systematically incorporated into these explicit algebraic stress models by a simple readjustment of the coefficients. For homogeneous turbulent flows that are close to equilibrium, it will be shown that the results obtained with such models are virtually indistinguishable from those obtained using a full second-order closure model with the anisotropic dissipation rate model of Speziale and Gatski.[4] All of this extra turbulence physics is incorporated within the framework of a two-equation model that is not much more computationally expensive to implement than the standard K–ε model.

II. Theoretical Background

We will consider incompressible turbulent flows where the velocity v_i and kinematic pressure P are decomposed, respectively, into ensemble mean and fluctuating parts as follows:

$$v_i = \bar{v}_i + u_i, \qquad P = \bar{P} + p \tag{1}$$

In homogeneous turbulence, where all higher-order correlations are spatially uniform, the Reynolds stress tensor $\tau_{ij} \equiv \overline{u_i u_j}$ satisfies the transport equation[9]

$$\dot{\tau}_{ij} = -\tau_{ik}\frac{\partial \bar{v}_j}{\partial x_k} - \tau_{jk}\frac{\partial \bar{v}_i}{\partial x_k} + \Pi_{ij} - \varepsilon_{ij} \tag{2}$$

where

$$\Pi_{ij} \equiv \overline{p\left(\frac{\partial u_i}{\partial x_j} + \frac{\partial u_j}{\partial x_i}\right)}, \qquad \varepsilon_{ij} \equiv 2\nu\overline{\frac{\partial u_i}{\partial x_k}\frac{\partial u_j}{\partial x_k}}$$

are, respectively, the pressure-strain correlation and the dissipation rate tensor. Thus, in homogeneous turbulence, only Π_{ij} and ε_{ij} need to be modeled to achieve closure.

Speziale et al.[10] (SSG) showed that, for two-dimensional mean turbulent flows in equilibrium, the commonly used hierarchy of pressure-strain models simplifies to

$$\begin{aligned}\Pi_{ij} = {} & -C_1\varepsilon b_{ij} + C_2\varepsilon\left(b_{ik}b_{kj} - \tfrac{1}{3}b_{kl}b_{kl}\delta_{ij}\right) + C_3 K\bar{S}_{ij} \\ & + C_4 K\left(b_{ik}\bar{S}_{jk} + b_{jk}\bar{S}_{ik} - \tfrac{2}{3}b_{kl}\bar{S}_{kl}\delta_{ij}\right) \\ & + C_5 K\left(b_{ik}\bar{\omega}_{jk} + b_{jk}\bar{\omega}_{ik}\right)\end{aligned} \tag{3}$$

where

$$\bar{S}_{ij} = \frac{1}{2}\left(\frac{\partial \bar{v}_i}{\partial x_j} + \frac{\partial \bar{v}_j}{\partial x_i}\right), \qquad \bar{\omega}_{ij} = \frac{1}{2}\left(\frac{\partial \bar{v}_i}{\partial x_j} - \frac{\partial \bar{v}_j}{\partial x_i}\right)$$

$$b_{ij} = \frac{\tau_{ij} - \frac{2}{3}K\delta_{ij}}{2K}$$

are, respectively, the mean rate of strain tensor, the mean vorticity tensor, and the Reynolds stress anisotropy tensor; $K \equiv \frac{1}{2}\tau_{ii}$ is the turbulent kinetic energy. The SSG model[10] is a simple extension of Eq. (3) that is valid for moderate departures from equilibrium. It has been found that the nonlinear return term containing C_2 can be neglected without introducing an appreciable error.[7,10] With the choice of constants

$$C_1 = 6.80, \qquad C_2 = 0, \qquad C_3 = 0.36$$

$$C_4 = 1.25, \qquad C_5 = 0.40$$

in Eq. (3), excellent equilibrium values are obtained for the benchmark case of homogeneous shear flow. We refer to this as the linearized, equilibrium form of the SSG model.

The Kolmogorov assumption of local isotropy is typically invoked wherein it is assumed that[2,9]

$$\varepsilon_{ij} = \tfrac{2}{3}\varepsilon\delta_{ij} \tag{4}$$

Received Feb. 3, 1996; revision received June 16, 1996; accepted for publication June 25, 1996; also published in *AIAA Journal on Disc*, Volume 2, Number 1.

*Research Assistant, Department of Aerospace and Mechanical Engineering.

†Professor, Department of Aerospace and Mechanical Engineering. Member AIAA.

where $\varepsilon \equiv \frac{1}{2}\varepsilon_{ii}$ is the (scalar) turbulent dissipation rate. It is generally accepted that homogeneous turbulent flows, with constant mean velocity gradients, achieve equilibrium values for b_{ij} that are largely independent of the initial conditions. This is characterized by

$$\dot{b}_{ij} = 0$$

or, equivalently,

$$\dot{\tau}_{ij} = 2(\mathcal{P} - \varepsilon)b_{ij} + \tfrac{2}{3}(\mathcal{P} - \varepsilon)\delta_{ij} \tag{5}$$

where $\mathcal{P} \equiv -\tau_{ij}\partial\bar{v}_i/\partial x_j$ is the turbulence production. The substitution of Eqs. (3–5) into Eq. (2) yields an implicit algebraic system that can be solved by integrity bases methods. This solution, which has come to be referred to as an explicit algebraic stress model (ASM), is given in the equilibrium limit of homogeneous turbulence by[7]

$$\tau_{ij} = \frac{2}{3}K\delta_{ij} - \frac{3}{3 - 2\eta^2 + 6\xi^2}\left[\alpha_0\frac{K^2}{\varepsilon}\bar{S}_{ij} + \alpha_1\frac{K^3}{\varepsilon^2}\right.$$

$$\left.\times\,(\bar{S}_{ik}\bar{\omega}_{kj} + \bar{S}_{jk}\bar{\omega}_{ki}) - \alpha_2\frac{K^3}{\varepsilon^2}\left(\bar{S}_{ik}\bar{S}_{kj} - \frac{1}{3}\bar{S}_{kl}\bar{S}_{kl}\delta_{ij}\right)\right] \tag{6}$$

where

$$\alpha_0 = \left(\tfrac{4}{3} - C_3\right)g, \qquad \alpha_1 = \tfrac{1}{2}\left(\tfrac{4}{3} - C_3\right)(2 - C_5)g^2$$

$$\alpha_2 = \left(\tfrac{4}{3} - C_3\right)(2 - C_4)g^2, \qquad g = \left(\tfrac{1}{2}C_1 + \mathcal{P}/\varepsilon - 1\right)^{-1} \tag{7}$$

$$\eta = \frac{1}{2}\frac{\alpha_2}{\alpha_0}\frac{K}{\varepsilon}(\bar{S}_{ij}\bar{S}_{ij})^{\frac{1}{2}}, \qquad \xi = \frac{\alpha_1}{\alpha_0}\frac{K}{\varepsilon}(\bar{\omega}_{ij}\bar{\omega}_{ij})^{\frac{1}{2}}$$

and $\mathcal{P}/\varepsilon$ assumes its constant equilibrium value. When far from equilibrium, a singularity may arise since the denominator $(3-2\eta^2+6\xi^2)$ in Eq. (6) can vanish for sufficiently high strain rates η. Gatski and Speziale[7] introduced a regularized expression for $3/(3-2\eta^2+6\xi^2)$ that eliminated the singular behavior. However, that model is not formally valid for nonequilibrium turbulence—particularly in the rapid distortion limit.

Speziale and Xu[11] later introduced a formal Padé approximation that built in some limited consistency with Rapid Distortion Theory (RDT) for homogeneous shear flow. They rewrote Eq. (6) in the form

$$\tau_{ij} = \tfrac{2}{3}K\delta_{ij} - \alpha_0^*(K^2/\varepsilon)\bar{S}_{ij} - \alpha_1^*(K^3/\varepsilon^2)(\bar{S}_{ik}\bar{\omega}_{kj} + \bar{S}_{jk}\bar{\omega}_{ki})$$

$$+\alpha_2^*(K^3/\varepsilon^2)\left(\bar{S}_{ik}\bar{S}_{kj} - \tfrac{1}{3}\bar{S}_{kl}\bar{S}_{kl}\delta_{ij}\right) \tag{8}$$

and made use of the fact that in the short-time RDT solution ($\eta \to \infty$), K/K_0 remains of order 1. This implies that

$$\alpha_0^* \sim (1/\eta) \tag{9}$$

It is obvious that the equilibrium model (6) violates this constraint ($\alpha_0^* \sim 1/\eta^2$ instead). Speziale and Xu[11] then introduced a Padé approximation and obtained the expression

$$\alpha_0^* = \frac{(1 + 2\xi^2)(1 + 6\eta^5) + \frac{5}{3}\eta^2}{(1 + 2\xi^2)\left(1 + 2\xi^2 + \eta^2 + 6\beta_0\eta^6\right)}\alpha_0 \tag{10}$$

(with the constant $\beta_0 \approx 7$) to ensure asymptotic consistency and the proper energy growth rate in line with the RDT data. By a comparable Padé approximation, they also derived the expression

$$\alpha_i^* = \frac{(1 + 2\xi^2)(1 + \eta^4) + \frac{2}{3}\eta^2}{(1 + 2\xi^2)\left(1 + 2\xi^2 + \beta_i\eta^6\right)}\alpha_i \tag{11}$$

for $i = 1, 2$ (with $\beta_1 \approx 6$ and $\beta_2 \approx 4$), to establish consistency with the approach to a one component turbulence in the RDT limit of homogeneous shear flow. For near-equilibrium turbulent flows, Eq. (8) with Eqs. (10) and (11) yields results that are virtually indistinguishable from Eq. (6).

III. Anisotropic Dissipation

In a recent study, Speziale and Gatski[4] derived a modeled transport equation for ε_{ij} that is valid for homogeneous turbulence. By invoking the equilibrium limit where

$$\dot{d}_{ij} = 0 \tag{12}$$

for the anisotropy of dissipation d_{ij}, they obtained an algebraic system—analogous to that for algebraic stress models—that was solved by integrity bases methods. This ultimately led to the algebraic model[4]

$$d_{ij} = -2C_{\mu\epsilon}\left[\tau\bar{S}_{ij} - \frac{\left(\frac{7}{11}\alpha_3 + \frac{1}{11}\right)\tau^2}{C_{\epsilon 5} + \mathcal{P}/\varepsilon - 1}(\bar{S}_{ik}\bar{\omega}_{kj} + \bar{S}_{jk}\bar{\omega}_{ki})\right.$$

$$\left.+\frac{\left(\frac{30}{11}\alpha_3 - \frac{2}{11}\right)\tau^2}{C_{\epsilon 5} + \mathcal{P}/\varepsilon - 1}\left(\bar{S}_{ik}\bar{S}_{kj} - \tfrac{1}{3}\bar{S}_{mn}\bar{S}_{mn}\delta_{ij}\right)\right] \tag{13}$$

where

$$d_{ij} = \frac{\varepsilon_{ij} - \frac{2}{3}\varepsilon\delta_{ij}}{2\varepsilon} \tag{14}$$

is the anisotropy of dissipation and $\tau \equiv K/\varepsilon$ is the turbulent time scale. Here,

$$C_{\mu\epsilon} = \frac{1}{15(C_{\epsilon 5} + \mathcal{P}/\varepsilon - 1)}$$

$$\times\left[1 + 2\tau^2\left(\frac{\frac{7}{11}\alpha_3 + \frac{1}{11}}{C_{\epsilon 5} + \mathcal{P}/\varepsilon - 1}\right)^2\bar{\omega}_{mn}\bar{\omega}_{mn}\right.$$

$$\left.-\frac{2}{3}\tau^2\left(\frac{\frac{15}{11}\alpha_3 - \frac{1}{11}}{C_{\epsilon 5} + \mathcal{P}/\varepsilon - 1}\right)^2\bar{S}_{mn}\bar{S}_{mn}\right]^{-1} \tag{15}$$

and

$$C_{\epsilon 5} = 5.8, \qquad \alpha_3 = 0.6$$

are constants. This then yields the full dissipation rate tensor because, by definition,

$$\varepsilon_{ij} = \tfrac{2}{3}\varepsilon\delta_{ij} + 2\varepsilon d_{ij} \tag{16}$$

After introducing the anisotropic dissipation model for d_{ij} in Eq. (2), we can derive an algebraic stress model with anisotropic dissipation. Again, making use of the fact that $\dot{b}_{ij} = 0$ for equilibrium turbulent flows, the Reynolds stress transport equation (2) then reduces to

$$2(\mathcal{P} - \varepsilon)b_{ij} = -2K\left(b_{ik}\bar{S}_{jk} + b_{jk}\bar{S}_{ik} - \tfrac{2}{3}b_{mn}\bar{S}_{mn}\delta_{ij}\right)$$

$$-\tfrac{4}{3}K\bar{S}_{ij} - 2K(b_{ik}\bar{\omega}_{jk} + b_{jk}\bar{\omega}_{ik}) + \Pi_{ij} - 2\epsilon d_{ij} \tag{17}$$

The explicit ASM incorporating anisotropic dissipation, which is obtained from the solution of Eq. (17), after Eqs. (3) and (13) are implemented, is of the same general tensorial form as Eq. (6):

$$b_{ij} = G^{(1)}T_{ij}^{(1)} + G^{(2)}T_{ij}^{(2)} + G^{(3)}T_{ij}^{(3)} \tag{18}$$

where

$$T_{ij}^{(1)} = \bar{S}_{ij}, \qquad T_{ij}^{(2)} = \bar{S}_{ik}\bar{\omega}_{kj} + \bar{S}_{jk}\bar{\omega}_{ki}$$

$$T_{ij}^{(3)} = \bar{S}_{ik}\bar{S}_{kj} - \tfrac{1}{3}\bar{S}_{mn}\bar{S}_{mn}\delta_{ij}$$

are the integrity bases. The solution is given by

$$G^{(1)} = \frac{1}{2}\alpha_0\tau\left[\frac{-1 - A_1 + \frac{1}{3}\eta^2 A_3 + 2\xi^2 A_2}{1 - \frac{2}{3}\eta^2 + 2\xi^2}\right]$$

$$G^{(2)} = \frac{1}{2}\alpha_1\tau^2\left[\frac{-1 - A_1 - A_2 + \frac{1}{3}\eta^2(A_3 + 2A_2)}{1 - \frac{2}{3}\eta^2 + 2\xi^2}\right] \quad (19)$$

$$G^{(3)} = \frac{1}{4}\alpha_2\tau^2\left[\frac{2 - A_3 + 2A_1 - 2\xi^2(A_3 + 2A_2)}{1 - \frac{2}{3}\eta^2 + 2\xi^2}\right]$$

where

$$A_1 = -\frac{4C_{\mu\epsilon}}{\frac{4}{3} - C_3}$$

$$A_2 = \frac{2}{g\left(\frac{4}{3} - C_3\right)(2 - C_5)}\frac{4C_{\mu\epsilon}\left(\frac{7}{11}\alpha_3 + \frac{1}{11}\right)}{(C_{\epsilon 5} + \mathcal{P}/\varepsilon - 1)}$$

$$A_3 = -\frac{2}{g\left(\frac{4}{3} - C_3\right)(2 - C_4)}\frac{4C_{\mu\epsilon}\left(\frac{30}{11}\alpha_3 - \frac{2}{11}\right)}{(C_{\epsilon 5} + \mathcal{P}/\varepsilon - 1)}$$

Equivalently, from Eq. (18) we have

$$\tau_{ij} = \tfrac{2}{3}K\delta_{ij} + 2K\left[G^{(1)}T_{ij}^{(1)} + G^{(2)}T_{ij}^{(2)} + G^{(3)}T_{ij}^{(3)}\right] \quad (20)$$

which is obviously of the same tensorial form as Eq. (6)—only the coefficients are different.

The factor $1/(1 - \frac{2}{3}\eta^2 + 2\xi^2)$ in Eq. (19) can be regularized in the same general way as discussed earlier to ensure the correct asymptotic behavior in the RDT limit. The standard explicit ASM given in Eq. (6) is then recovered in the limit as $C_{\mu\epsilon}$ (and, hence, A_1, A_2, and A_3) $\to 0$. Anisotropies in the dissipation rate are then accounted for simply through a systematic readjustment of the coefficients.

IV. Results and Discussion

The anisotropic dissipation rate model has been tested in detail by Speziale and Gatski[4] within the context of a full second-order closure, which will not be repeated here. Our purpose in this Note is to simply demonstrate that, for homogeneous turbulent flows close to equilibrium, the new explicit ASM with anisotropic dissipation yields results that are indistinguishable from the full second-order closure, with anisotropic dissipation, on which it is based.

The new explicit ASM with anisotropic dissipation derived herein is solved with a modeled transport equation for the turbulent dissipation rate that is of the form[4]

$$\dot{\varepsilon} = C_{\epsilon 1}^*(\varepsilon/K)\mathcal{P} - C_{\epsilon 2}(\varepsilon^2/K) \quad (21)$$

for homogeneous turbulence. Here

$$C_{\epsilon 1}^* = 1.26 + \frac{2(1+\alpha)}{15C_\mu} \times \left[\frac{C_{\epsilon 5} + 2C_\mu\eta^2 - 1}{\left(C_{\epsilon 5} + 2C_\mu\eta^2 - 1\right)^2 + 2\beta_1^2\xi^2 - \frac{2}{3}\beta_2^2\eta^2}\right] \quad (22)$$

where

$$\alpha = \tfrac{3}{4}\left(\tfrac{14}{11}\alpha_3 - \tfrac{16}{33}\right)$$

$$\beta_1 = \tfrac{7}{11}\alpha_3 + \tfrac{1}{11}, \qquad \beta_2 = \tfrac{15}{11}\alpha_3 - \tfrac{1}{11}$$

and C_μ and $C_{\epsilon 2}$ are constants that assume the approximate values of 0.09 and 1.83, respectively. In Eq. (22), $\eta \equiv (\bar{S}_{ij}\bar{S}_{ij})^{1/2}\tau$ and $\xi \equiv (\bar{\omega}_{ij}\bar{\omega}_{ij})^{1/2}\tau$. The effects of anisotropic dissipation are rigorously accounted for in Eq. (21) through the variable coefficient $C_{\epsilon 1}^*$. For inhomogeneous turbulent flows, a gradient transport term of the standard form

$$\frac{\partial}{\partial x_i}\left(\frac{\nu_T}{\sigma_\epsilon}\frac{\partial \varepsilon}{\partial x_i}\right)$$

is added to the right-hand side of Eq. (21) to account for turbulent diffusion.

Table 1 Equilibrium values for homogeneous shear flow[a]

Equilibrium values	Explicit ASM	Full closure	DNS
b_{11}	0.204	0.205	0.215
b_{12}	−0.150	−0.150	−0.158
b_{22}	−0.148	−0.147	−0.153
b_{33}	−0.056	−0.058	−0.062
SK/ε	5.98	5.96	5.70

[a]Comparison of the new explicit ASM incorporating anisotropic dissipation with the DNS of Rogers et al.[12] and a full Reynolds stress closure with anisotropic dissipation (containing the linearized SSG second-order closure and the anisotropic dissipation rate model of Speziale and Gatski[4]).

To demonstrate the ability of the new model to properly capture the physics of the more complicated full second-order closure with anisotropic dissipation, we will present a simple example of a benchmark turbulent flow. In Table 1, we compare the equilibrium results of the new explicit ASM for homogeneous shear flow with the predictions of the linearized SSG second-order closure incorporating the anisotropic dissipation rate model of Speziale and Gatski.[4] These calculations were conducted with a fourth-order accurate Runge–Kutta numerical integration scheme. It is clear from these calculations that the new explicit ASM yields results that are virtually identical to the results of the full second-order closure with anisotropic dissipation and compare favorably with the direct numerical simulation (DNS) results of Rogers et al.[12] This definitively demonstrates the power of the new model to yield results that are indistinguishable from a full second-order closure—with anisotropic dissipation—for turbulent flows that are close to equilibrium. All of this at a small fraction of the computer costs. Although the effects of anisotropic dissipation are not that significant for this case, they can be important in other flows of engineering interest as alluded to earlier. We consider this to be a highly promising new approach for such flows that can have important engineering applications and, thus, warrants further study.

Acknowledgments

This research was supported by the U.S. Office of Naval Research under Grant N00014-94-1-0088, L. P. Purtell, Program Officer. Partial support was also provided by the NASA Langley Research Center through Contract NAG1-1712. The authors are indebted to T. B. Gatski (NASA Langley Research Center) for some helpful comments.

References

[1]Mansour, N. N., Kim, J., and Moin, P., "Reynolds Stress and Dissipation Rate Budgets in Turbulent Channel Flow," *Journal of Fluid Mechanics*, Vol. 194, 1988, pp. 15–44.

[2]Durbin, P. A., and Speziale, C. G., "Local Anisotropy in Strained Turbulence at High Reynolds Numbers," *Journal of Fluids Engineering*, Vol. 113, No. 4, 1991, pp. 707–709.

[3]Speziale, C. G., Raj, R., and Gatski, T. B., "Modeling the Dissipation Rate in Rotating Turbulent Flows," *Studies in Turbulence*, edited by T. B. Gatski, S. Sarkar, and C. G. Speziale, Springer–Verlag, New York, 1992, pp. 129–151.

[4]Speziale, C. G., and Gatski, T. B., "Analysis and Modeling of Anisotropies in the Dissipation Rate of Turbulence," Dept. of Aerospace and Mechanical Engineering, TR AM-95-026, Boston Univ., Boston, MA, Oct. 1995.

[5]Oberlack, M., "Non-Isotropic Dissipation in Non-Homogeneous Turbulence," *Journal of Fluid Mechanics* (submitted for publication).

[6]Hallbäck, M., Groth, J., and Johansson, A. V., "An Algebraic Model for Nonisotropic Turbulent Dissipation Rate in Reynolds Stress Closures," *Physics of Fluids A*, Vol. 2, No. 10, 1990, pp. 1859–1866.

[7]Gatski, T. B., and Speziale, C. G., "On Explicit Algebraic Stress Models for Complex Turbulent Flows," *Journal of Fluid Mechanics*, Vol. 254, 1993, pp. 59–78.

[8]Abid, R., Morrison, J. H., Gatski, T. B., and Speziale, C. G., "Prediction of Complex Aerodynamic Flows with Explicit Algebraic Stress Models," AIAA Paper 96-0565, Jan. 1996.

[9]Hinze, J. O., *Turbulence*, McGraw–Hill, New York, 1975, Chap. 1.

[10]Speziale, C. G., Sarkar, S., and Gatski, T. B., "Modeling the Pressure-Strain Correlation of Turbulence: An Invariant Dynamical Systems Approach," *Journal of Fluid Mechanics*, Vol. 227, 1991, pp. 245–272.

[11]Speziale, C. G., and Xu, X.-H., "Towards the Development of Second-Order Closure Models for Non-Equilibrium Turbulent Flows," *Proceedings of the 10th Symposium on Turbulent Shear Flows*, Vol. 3, Pennsylvania State Univ., State College, PA, 1995, pp. 23.7–23.12.

[12]Rogers, M. M., Moin, P., and Reynolds, W. C., "The Structure and Modeling of the Hydrodynamic and Passive Scalar Fields in Homogeneous Turbulent Shear Flow," Stanford Univ., TR TF-25, Stanford, CA, Aug. 1986.

Numerical Simulation of Viscous Flow over Rotors Using a Distributed Computing Strategy

Ashok Bangalore,* Ralph L. Latham,† and Lakshmi N. Sankar‡
Georgia Institute of Technology, Atlanta, Georgia 30332-0150

Introduction

SCIENTIFIC computing using parallel computers has been a topic of active research for the past several years. Several parallel supercomputers are being used today, such as the Intel Paragon, Connection Machine CM-5, MASPAR, KSR, and Cray Y/MP systems. The recent versions are multiple instruction multiple data machines, and they differ from each other in the number of processors used (16–64,000), the computational power of the individual processors, and the strategy for passing messages and information between processors. In general, the computer codes must be tailored to individual architecture for maximum performance, although common machine-independent programming practices using Fortran-90 and High Performance Fortran are evolving. The parallel supercomputers are expensive and usually are used heavily. Typical turnaround times for a computational fluid dynamics (CFD) application may vary from one day to several days. Turnaround times of this order and the high equipment cost of these machines make them impractical for small research labs, universities, and many aerospace firms.

A new, inexpensive way of parallel computing, using a network of heterogeneous computers known as distributed computing, is available.[1] Many of these workstations are idle after work hours, because each of them is not individually big enough to solve large-scale problems. Distributed computing allows this idle time to be used effectively. For the distributed computing to be effective, standard, portable, efficient methods for interprocessor communications are needed. In the present study, interprocessor communications was achieved through a software called Parallel Virtual Machine (PVM), which is being developed by the joint efforts of Oak Ridge National Laboratory and Emory University.[2]

Many researchers have begun to study the use of PVM in distributed CFD applications. For example, Smith and Pallis[3] have implemented the PVM software to solve the Navier–Stokes equations using MEDUSA, an overset grid flow solver on a cluster of heterogeneous workstations at NASA Ames Research Center. They have reported significant gain in computation time by using the PVM software. They also point out the economics of using workstations as opposed to using supercomputers. More recently, Weed and Sankar[4] ported a multiblock Euler/Navier–Stokes code (TEAM) to a distributed network and reported significant gain in computation time when solving large-scale problems.

PVM Implementation

The basic idea in implementing PVM software in the existing Navier–Stokes solver[5,6] is to divide the computational domain into smaller blocks and solve each block of grid points on a different processor. The original Navier–Stokes solver is an unsteady, three-dimensional finite volume-based code and has been extensively documented in Ref. 5. In the present application, the computational grid is a C-H grid around the fixed wing or rotor blade with 121 points in the streamwise direction, 28 points in the spanwise direction, and 41 points in the normal direction. The complete domain is divided into two or three spanwise zones, depending on the number of processors used. Splitting the domain in the spanwise direction is efficient and convenient because the spanwise direction is treated explicitly. Figure 1 shows schematically the division of spanwise zones. Using the PVM message-passing routines, the flow data are sent from the slave processes to the master process at each time step. Also, updated interface data are sent to the slaves from the master process using the PVM routines.

Results and Discussion

Speedup and Performance

The virtual machine network used in the present work consisted of three Hewlett-Packard (HP) Apollo workstations: two model 720 and one model 730. The benchmark and performance monitoring for the present Navier–Stokes code using the PVM software was done on this network with no other user processes running on the machines. The workload on the machines was near zero and this gave a realistic figure of speedup obtained by using the PVM software.

The CPU and the elapsed time during each iteration are obtained using the time ( ) function call provided in the Fortran library. The time ( ) function gives the elapsed time rounded to the nearest second. This level of accuracy was adequate for the present application because the computation time required per time step was of the order of 10–20 s. The amount of message passing between the master and the slave processes was about 452 kB of flow data per iteration. The actual communication time taken for this particular packet of data was less than 0.1 s on the present ethernet network. This indicated that the latency of the network was a very small percentage of the total wait time of the processes.

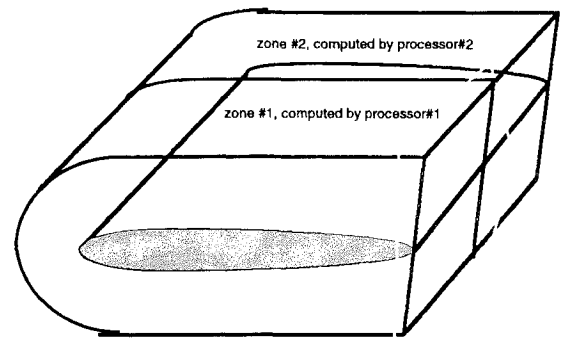

Fig. 1 Spanwise division of the domain.

Received Nov. 18, 1994; presented as Paper 95-0575 at the AIAA 33rd Aerospace Sciences Meeting, Reno, NV, Jan. 9–12, 1995; revision received Nov. 15, 1995; accepted for publication Jan. 12, 1996.

*Graduate Research Assistant, School of Aerospace Engineering; currently Postdoctoral Researcher, 233 Hammond Building, Pennsylvania State University, University Park, PA 16802.

†Research Engineer, School of Aerospace Engineering.

‡Professor, School of Aerospace Engineering. Senior Member AIAA.